Microcontact and Macrocontact Angles and the Drop Stability on a Bare Surface

Gersh O. Berim and Eli Ruckenstein*

Department of Chemical and Biological Engineering, State University of New York at Buffalo, Buffalo, New York 14260

Received: August 10, 2004

The microscopic approach of ref 1 regarding the shape and stability of a liquid drop on a bare solid surface is extended to include the structuring of the liquid near the solid surface. It is supposed that the liquid molecules near the solid form a monolayer, which is characterized by a surface number density and short- and long-range interactions with the solid. The rest of the drop is considered as a continuous medium with only long-range interactions with the solid. Two kinds of droplets, cylindrical (two-dimensional) and axisymmetrical (three-dimensional), were examined for two types of interaction potentials similar to the London−van der Waals and the Lennard-Jones ones. The microcontact angle, θ_0, that the drop profile makes with the solid surface is dependent on the microscopic parameters of the model (strength of intermolecular interactions, densities of liquid and solid phases, hard core radius, etc.), whereas in the previous continuum picture of ref 1, it was constant and equal to 180°. All drop characteristics, such as stability, shape, and macroscopic contact angle, become functions of θ_0 and a certain parameter a dependent on the model interaction parameters. There are two domains in the plane θ_0-a for the drop stability, separated by a critical curve. In the first domain, the drop can have any height, h_m, at its apex and is always stable. In the second domain, h_m is limited by a critical value, h_c, which depends on a and θ_0, and drops with $h_m > h_c$ cannot exist. The drop shape depends on whether the point (θ_0, a) on the θ_0-a plane is far from the critical curve or near it. In the first case, the drop profile has a large circular part, while in the second case, the shape is almost planar. By extrapolating for sufficiently large drops the spherical part to the solid surface, one can obtain the macroscopic (apparent) contact angle, which is accessible experimentally. In the region near the solid surface, the tangent to the profile makes with the solid surface an angle that varies rapidly between the microcontact angle, θ_0, and the macroscopic contact angle,θ_m.

I. Introduction

The microscopic theory that describes a liquid drop on a bare solid substrate, which was developed in refs 1−3, is based on a continuum picture implying that the drop is spatially homogeneous and can be characterized by a constant number density. Equations for the drop profile were obtained either by considering the mechanical equilibrium of the molecules on the drop surface[2,3] or through the variational minimization of the total potential energy of the drop.[1] In the framework of the latter approach, it was shown[1] that the height h_m of the drop at its apex can have, even in the absence of gravity, any value only if a parameter a, which is a combination of the interaction parameters characterizing the interactions between the molecules of the liquid as well as between the molecules of the solid and liquid, is less than a critical value, a_c. For $a > a_c$, the droplet height, h_m, is limited by a critical value, h_c, which depends on a. Were a droplet with a height larger than h_c to be artificially created, it would transform into a droplet with a new height less than h_c. If h_m is close to h_c, the droplet will have a planar shape.

Among the results, the theory of ref 1 provided a constant value $\theta_0 = 180°$ for the microcontact angle, which the drop profile makes with the solid surface. Whereas the macroscopic (apparent) contact angle, θ_m, which was defined for sufficiently large drops using a continuation of the circular part of the drop profile, was dependent on the intermolecular interactions and is accessible experimentally, the angle θ_0 was constant. A possible reason for such a behavior of the microcontact angle might be the inadequacy of the continuum picture for the description of the drop. Indeed, the assumption of drop homogeneity may be not valid, especially in the vicinity of the solid surface where the interactions between the molecules of liquid and solid are both short- and long-range. Hence, near the solid surface, a layer of liquid molecules can appear that is beyond the continuum picture.

In this paper, the microscopic approach of refs 1−3 is modified to include the characteristics of the liquid near the solid surface. It is shown that in this case the microcontact angle θ_0 at the solid surface becomes a function of the parameters of the intermolecular interactions. The dependence of the microcontact angle on the parameters of intermolecular interactions affects both the shape and the stability of the drop. For example, in the new picture the above-mentioned quantities, a_c and h_c, become dependent on the microcontact angle, θ_0.

It was also shown previously[1−3] that the profile of a liquid drop on a solid substrate exhibits a rapid variation of curvature in a small region (∼10−100 Å) near the surface, due to the rapid variation of the interactions between molecules of liquid and solid. Because of its small size, this region and, in particular,

* To whom correspondence should be addressed. Electronic mail: feaeliru@acsu.buffalo.edu. Phone number: (716)645-2911, ext. 2214. Fax: (716)645-3822.

10.1021/jp0464019 CCC: $27.50
Published on Web 11/19/2004

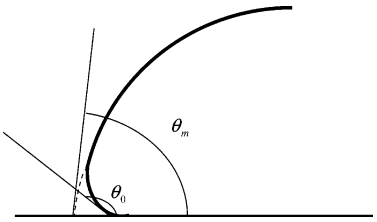

Figure 1. Microcontact angle θ_0 and macroscopic (apparent) contact angle θ_m. The latter angle is defined using a continuation of the circular part of the drop profile.

the microcontact angle θ_0 are practically undetectable in macroscopic experiments, while the macroscopic contact angle, which represents an extrapolation of the circular part of the drop profile to the solid surface, is a measurable quantity (see Figure 1).

In section II, the interaction potentials between the molecules of liquid and solid are introduced and a general form of the total potential energy is derived by taking into account the presence of a special liquid layer near the solid surface. The application of these expressions to a cylindrical droplet is considered in section III and that for an axisymmetrical droplet in section IV.

II. Basic Equation

A. Potentials. Assuming that the interaction of the drop molecules with the molecules of the surrounding vapor is negligible, two potentials, $\phi_{LL}(r)$ and $\phi_{LS}(r)$ are considered, which describe, respectively, the interaction of a molecule of a liquid drop with the other molecules of the drop and that with the molecules of the solid (r is the distance between the centers of the interacting molecules). For a variety of liquids, the potential $\phi_{LL}(r)$ can be considered to be a combination between a London−van der Waals (LvdW) attraction and a rigid core repulsion[4]

$$\tilde{\phi}_{LL}(r) = \begin{cases} -\epsilon'_{LS}\left(\dfrac{\sigma'_{LL}}{r}\right)^6 & r \geq \sigma'_{LL} \\ \infty & r < \sigma'_{LL} \end{cases} \quad (1)$$

where σ'_{LL} and $\epsilon'_{LL} > 0$ are the size of the repulsive core and an interaction constant, respectively. The calculation of the potential energy of a liquid drop based on potential eq 1 is a complicated problem. To avoid difficulties, a more simple square-well potential

$$\phi_{LL}(r) = \begin{cases} -\epsilon_{LL} & r \leq \eta \\ 0 & r > \eta \end{cases} \quad (2)$$

will be used, where η is the radius of the so-called interaction sphere[1] and ϵ_{LL} characterizes the strength of the interactions. Despite its oversimplified form, such a potential is a reasonable approximation for the qualitative understanding of various phenomena.[5] With appropriate choices for the parameters ϵ_{LL} and η, the potential eqs 2 and 1 can provide equal values for at least some of the physical characteristics of the system. As an example, let us compare the total potential energy of a molecule in the bulk of a homogeneous liquid calculated using potential eq 1 to that obtained using potential eq 2. The first potential energy, ϕ'_1, is given by

$$\phi'_1 = \int_0^{2\pi} d\phi \int_0^{\pi} d\theta \sin\theta \int_{\sigma'_{LL}}^{\infty} \phi'_{LL}(r)\rho_L r^2 dr = -\frac{4}{3}\pi\sigma'^3_{LL}\epsilon'_{LL}\rho_L \quad (3)$$

where ρ_L is the liquid density. The second potential energy, ϕ_1, is proportional to the volume of the interaction sphere and is equal to

$$\phi_1 = -\frac{4}{3}\pi\eta^3\epsilon_{LL}\rho_L \quad (4)$$

Comparing eqs 3 and 4, one arrives at an expression connecting the parameters of the two potentials

$$\frac{\epsilon_{LL}}{\epsilon'_{LL}} = \left(\frac{\sigma'_{LL}}{\eta}\right)^3 \quad (5)$$

In particular, one of the possible choices of the parameters ϵ_{LL} and η is $\epsilon_{LL} = \epsilon'_{LL}$ and $\eta = \sigma'_{LL}$.

The interaction potential $\phi_{LS}(r)$ will be represented as the sum of two components, $\phi^l_{LS}(r)$ and $\phi^s_{LS}(r)$, related to the long-range and the short-range (acid−base) interactions between the liquid and solid. The long-range potential is chosen in the form

$$\phi^l_{LS}(r) = \begin{cases} \epsilon_{LS}\left[k_\phi\left(\dfrac{\sigma_{LS}}{r}\right)^{12} - \left(\dfrac{\sigma_{LS}}{r}\right)^6\right] & r \geq \sigma_{LS} \\ \infty & r < \sigma_{LS} \end{cases} \quad (6)$$

where $k_\phi = 0$ or 1, σ_{LS} and $\epsilon_{LS} > 0$ are, respectively, the size of the repulsive core and the interaction constant of the liquid−solid interactions. For $k_\phi = 0$, one recovers the LvdW potential and for $k_\phi = 1$ and $r \geq \sigma_{LS}$ the Lennard-Jones (LJ) potential. In what follows, σ_{LS} is used as unit of length. In real systems, σ_{LS} is of the order of several angstroms.[6]

Assuming pairwise additivity, the potential of a liquid molecule interacting with a semi-infinite solid through the long-range interactions can be written as

$$\Phi^l_{LS}(h) = \frac{\pi}{6}\epsilon_{LS}\rho_S\sigma^3_{LS}\left[\frac{2}{15}k_\phi\left(\frac{\sigma_{LS}}{h+\sigma_{LS}}\right)^9 - \left(\frac{\sigma_{LS}}{h+\sigma_{LS}}\right)^3\right], \quad h \geq 0 \quad (7)$$

where ρ_S is the constant number density of molecules in the solid and $h + \sigma_{LS}$ is the distance of the center of the molecule of liquid from the first layer of solid atoms ($h = 0$ corresponds to the centers of the layer of liquid molecules on the solid surface).

The short-range potential, $\phi^s_{LS}(r)$, accounts for the acid−base interactions, which can be attractive as well as repulsive.[7] It is assumed that $\phi^s_{LS}(r)$ decays exponentially and can be considered zero at distances larger than $l_0 \approx 1$ nm.[7,8] It will be supposed that the potential energy $\Phi^s_{LS}(h)$ of a liquid molecule due to the short-range interactions has the value $-\epsilon^s_{LS}$ for the molecules of the first layer of liquid near the solid surface ($h = 0$) and is equal to zero for all other molecules. The distance of the first layer of liquid molecules from the solid surface is assumed to be equal to the hard core radius, σ_{LS}, of the potential eq 6. As a result, the potential $\Phi^s_{LS}(h)$ is given by

$$\Phi^s_{LS}(h) = \begin{cases} -\epsilon^s_{LS} & h = 0 \\ 0 & h > 0 \end{cases} \quad (8)$$

Note that the interaction constant ϵ^s_{LS} can be positive or negative depending on the system. The microscopic calculation of ϵ^s_{LS} is a separate issue.

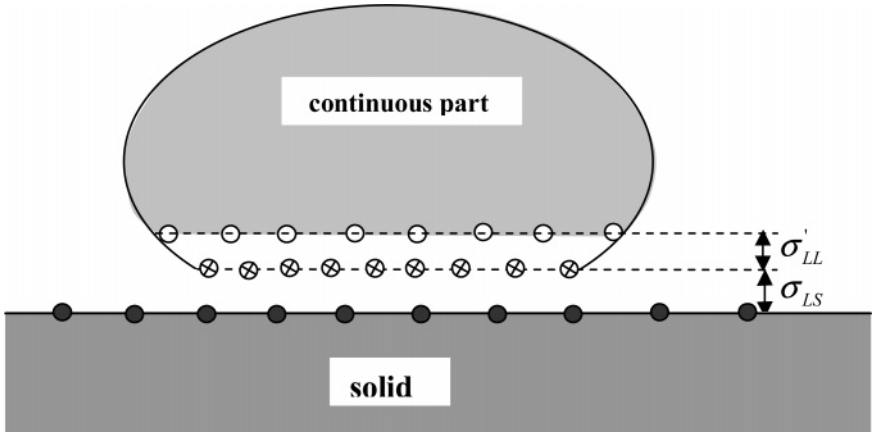

Figure 2. The cross-section of a drop on a solid surface. The filled and crossed circles represent the molecules of the solid surface and the molecules of the first (nearest to the solid surface) layer of liquid molecules, respectively. Beginning with the second layer (open circles), the liquid is considered as a continuous medium.

The potential eqs 7 and 8 have to be combined to provide the total potential $\Phi_{LS}(h)$ of a molecule of liquid interacting with a semi-infinite solid

$$\Phi_{LS}(h) = \begin{cases} \Phi^{l}_{LS}(0) + \Phi^{s}_{LS}(0) & h = 0 \\ \Phi^{l}_{LS}(h) & h > 0 \end{cases} \tag{9}$$

The most frequently used model for the theoretical description of liquid drops is a continuum model, which considers the liquid as a continuous medium characterized by a macroscopic number density, ρ_L, the latter being, in general, a function of the space coordinates. Such a description implies that all interactions change slowly for distances comparable with the intermolecular distances in the liquid. This assumption is not valid in the very close vicinity of the solid surface where the liquid−solid interactions (long- as well as short-range) change rapidly with the moving away from the solid surface. For example, the potential $\Phi_{LS}{}^{l}(h)$ (for $k_\phi = 0$ and $\sigma_{LS} \simeq \sigma'_{LL}$) is 8-fold smaller for the molecules of the second layer of liquid than for the molecules of the first layer. Due to the strong liquid−solid interactions, the liquid molecules nearest to the solid surface are arranged in a layer "stuck" to the solid surface, which will be assumed to be a monolayer. The rest of the drop is assumed to be a continuous medium of constant density (see Figure 2).

B. Potential Energy of a Drop. The total potential energy of a drop (the gravity is neglected)

$$U_{total} = U_{LL} + U_{LS} \tag{10}$$

consists of a potential energy U_{LL} due to the interactions of the molecules of liquid between themselves and a potential energy U_{LS} due to the interactions between the molecules of liquid and the molecules of solid. The presence of a liquid monolayer on the solid surface will be taken into account during the calculation of U_{LS}. In the calculation of U_{LL}, the deviation from the continuum model is neglected.

The energy U_{LL} for a constant number density ρ_L and the interaction potential eq 2 was calculated in ref 1, and the result has the form

$$U_{LL} = -\frac{2}{3}\pi\eta^3\rho_L{}^2\epsilon_{LL}V + \frac{1}{8}\pi\eta^4\rho_L{}^2\epsilon_{LL}S \tag{11}$$

where V and $S = S_{LV} + S_{LS}$ are the total volume and surface of the drop, respectively, the latter including the areas of the liquid−vapor (S_{LV}) and liquid−solid (S_{LS}) interfaces. The two terms in the right-hand side of eq 11 represent the bulk and liquid/vapor surface energy of the droplet. The coefficient multiplying the area S can be considered as a microscopic expression for the surface tension γ_{lv} of the liquid/vapor interface ($\gamma_{lv} = {}^1/_8\pi\eta^4\rho_L{}^2\epsilon_{LL}$).

To calculate the interaction energy U_{LS}, it will be supposed that the molecules of liquid near the planar solid surface form a monolayer with a constant surface number density, ρ_{LS}, separated from the solid surface by the distance σ_{LS}. The molecules of that layer are affected by both long-range and short-range interactions with the solid, which are represented by potential eq 9 for $h = 0$. The continuous part of the drop is separated from the first layer by the distance $\sigma'_{LL} \approx \eta$ and its molecules do not exhibit short-range interactions.

Under the above assumptions, the energy U_{LS} is given by

$$U_{LS} = \rho_{LS}\Phi_{LS}(0)S_{LS} + \int_{V_{cont}} \rho_L \Phi^{l}_{LS}(h)\, dV \tag{12}$$

where S_{LS} is the contact area between the droplet and the solid, and V_{cont} denotes the volume of the continuous part of the droplet. The latter can be represented as the difference between the drop volume V and the volume V_g of the gap between the first layer and the continuous part of the droplet, which is approximately equal to $V_g = \sigma'_{LL}S_{LS}$,, that is,$V_{cont} = V - S_{LS}\sigma'_{LL}$. Then the second term in the right-hand side of eq 12 can be written as

$$\int_{V_{cont}} \rho_L \Phi^{l}_{LS}(h)\, dV = \int_{V} \rho_L \Phi^{l}_{LS}(h)\, dV - \int_{V_s} \rho_L \Phi^{l}_{LS}(h)\, dV$$

$$\simeq \int_{V} \rho_L \Phi^{l}_{LS}(h)\, dV - \rho_L \sigma'_{LL} \Phi^{l}_{LS}(\sigma'_{LL}) S_{LS} \tag{13}$$

Consequently,

$$U_{LS} \simeq \int_{V} \rho_L \Phi^{l}_{LS}(h)\, dV + [\rho_{LS}\Phi_{LS}(0) - \rho_L \sigma'_{LL} \Phi^{l}_{LS}(\sigma'_{LL})] S_{LS} \tag{14}$$

Equations 11 and 14 provide a basis for the analysis of the drop characteristics (shape, stability, etc.) using the minimization of the total potential energy, eq 10. Below, these characteristics will be examined separately for cylindrical and axisymmetrical droplets.

III. Cylindrical Droplet

A. Equations for the Profile and the Microcontact Angle. Let us assume that a cylindrical liquid drop is extended along

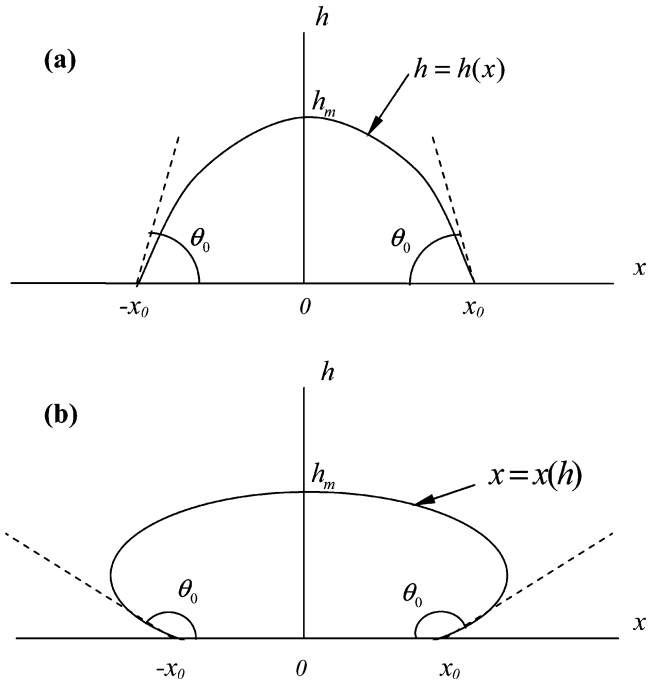

Figure 3. Two characteristic profiles of a cylindrical droplet: (a) microcontact angle θ_0 smaller than 90°; (b) θ_0 larger than 90°. The *y*-axis is normal to the plane of the figure.

the *y*-axis and has a cross-section symmetrical with respect to the *h*-axis. Depending on the value of the microcontact angle, the drop profile can have the shapes presented in Figure 3. It is usual practice[9−11] to describe the drop profile through the classical augmented Young−Laplace differential equation, which for a cylindrical droplet has the form

$$\frac{h_{xx}}{(1+h_x^{\,2})^{3/2}} + \Pi(h)/\gamma_{lv} = -p_c/\gamma_{lv} \tag{15}$$

where $h \equiv h(x)$ is the drop thickness, the subscript of h denotes the derivative with respect to the corresponding variable, γ_{lv} is the bulk liquid/vapor surface tension, $\Pi(h)$ is the disjoining pressure originating from the liquid−solid and liquid−liquid interactions, and p_c is the capillary pressure. The disjoining pressure can be obtained from the potential interaction energy, $P(h)$, that is $\Pi(h) = -(\mathrm{d}/\mathrm{d}h)P(h)$. However, eq 15 describes only the profiles for which $\theta_0 \le 90°$ (Figure 3a), because for $\theta_0 > 90°$ the function $h(x)$ is not unique for $|x| > x_0$, where x_0 is the abscissa of the leading edge of the droplet. To include both shapes (Figure 3, parts a and b) into consideration, the equation of the droplet profile is chosen in the form $x = x(h)$, and only the part of the profile for which $x \ge 0$ will be considered further. With such a choice, one can write (all quantities are calculated per unit length of the droplet in the *y*-direction)

$$V = 2\int_0^{h_m} x\,\mathrm{d}h, \quad S_{LV} = 2\int_0^{h_m}\sqrt{1+x_h^{\,2}}\,\mathrm{d}h$$

$$S_{LS} = 2x(0) = -2\int_0^{h_m} x_h\,\mathrm{d}h,$$

$$\int_V \rho_L \Phi_{LS}^{l}(h)\,\mathrm{d}V = 2\rho_L\int_0^{h_m}\Phi_{LS}^{l}(h)x\,\mathrm{d}h \tag{16}$$

where the subscript of x denotes the derivative with respect to the corresponding variable, h_m is the droplet height, and $x(0) = -\int_0^{h_m} x_h\,\mathrm{d}h$ follows from the obvious expression $x(h_m) = 0$. The total potential energy, eq 10, per unit length is given by

$$U_{total} = \int_0^{h_m} f(h,x,x_h)\,\mathrm{d}h \tag{17}$$

where

$$f(h,x,x_h) = \frac{1}{4}\pi\eta^4\rho_L^{\,2}\epsilon_{LL}\{[-a_0 + a_1\Phi_{LS}^{l}(h)]x + \sqrt{1+x_h^{\,2}} - bx_h\} \tag{18}$$

$$a_0 = \frac{16}{3\eta}, \quad a_1 = \frac{8}{\pi\eta^4\rho_L\epsilon_{LL}} \tag{19}$$

and

$$b = 1 + \frac{8\sigma'_{LL}}{\pi\rho_L\eta^4\epsilon_{LL}}\left[\frac{\rho_{LS}}{\rho_L\sigma'_{LL}}\Phi_{LS}(0) - \Phi_{LS}^{l}(\sigma'_{LL})\right] \tag{20}$$

In eq 20, according to eqs 9, 8, and 7

$$\Phi_{LS}(0) = \frac{\pi}{6}\epsilon_{LS}\rho_S\sigma_{LS}^{\,3}\left(\frac{2}{15}k_\phi - 1\right) - \epsilon_{LS}^{s} \tag{21}$$

and

$$\Phi_{LS}^{l}(\sigma'_{LL}) = \frac{\pi}{6}\epsilon_{LS}\rho_S\sigma_{LS}^{\,3}\left[\frac{2}{15}k_\phi\left(\frac{\sigma_{LS}}{\sigma'_{LL}+\sigma_{LS}}\right)^9 - \left(\frac{\sigma_{LS}}{\sigma'_{LL}+\sigma_{LS}}\right)^3\right] \tag{22}$$

If one uses as a constraint the given volume V of the drop, then the equation of the drop profile can be obtained by the variational minimization of the functional

$$\int_0^{h_m} f(h,x,x_h)\,\mathrm{d}h + 2\lambda\int_0^{h_m} x\,\mathrm{d}h \tag{23}$$

where λ is a Lagrange multiplier for the drop volume. The functional eq 23 can be rewritten in the following more convenient form

$$\int_0^{h_m} F(h,x,x_h)\,\mathrm{d}h \tag{24}$$

where

$$F(h,x,x_h) = [\lambda_c + a_1\Phi_{LS}^{l}(h)]x + \sqrt{1+x_h^{\,2}} - bx_h$$

$$\lambda_c = 8\lambda/(\pi\eta^4\rho_L^{\,2}\epsilon_{LL}) - a_0 \tag{25}$$

The latter functional is obtained by dividing the functional eq 23 with the nonzero coefficient $\pi\eta^4\rho_L^{\,2}\epsilon_{LL}/4$.

Using the standard calculus of variations,[12] one can obtain the following differential equation for the profile:

$$\frac{x_{hh}}{(1+x_h^{\,2})^{3/2}} - a_1\Phi_{LS}^{l}(h) = \lambda_c \tag{26}$$

which coincides in form with the augmented Young−Laplace equation (eq 15) for cylindrical droplets. The first terms of eqs 26 and 15 represent the curvature $\kappa(h)$ of the profile, which in the considered case can be rewritten as

$$\kappa(h) = \lambda_c + a_1\Phi_{LS}^{l}(h) \tag{27}$$

with a curvature radius given by

$$R^{\mathrm{curv}}(h) = \frac{1}{|\kappa(h)|} \tag{28}$$

One can establish the following correspondence between the disjoining [$\Pi(h)$] and the capillary (p_c) pressures in eq 15 and the terms involved in eq 26:

$$\Pi(h)/\gamma_{lv} = -a_1\Phi^l_{LS}(h); \quad \lambda_c = -p_c/\gamma_{lv} \tag{29}$$

Because the apex of the droplet and the contact point of the profile with the solid should be located on the h- and x-axes, respectively, one can also write the so-called transversality conditions[12]

$$\frac{\partial}{\partial x_h}F(h,x,x_h)|_{h=0} = 0, \quad \left[F(h,x,x_h) - x_h\frac{\partial}{\partial x_h}F(h,x,x_h)\right]|_{h=h_m} = 0 \tag{30}$$

which provide the following two boundary conditions for eq 26

$$\frac{1}{\sqrt{1+x_h^2}}|_{h=h_m} = 0 \tag{31}$$

$$\frac{x_h}{\sqrt{1+x_h^2}}|_{h=0} = b \tag{32}$$

The first condition, eq 31, or, equivalently, $x_h|_{h=h_m} = \infty$ ($h_x|_{x=0} = 0$), reflects the fact that the tangent to the drop profile at its apex should be parallel to the solid surface. The second condition, eq 32, provides an expression for the microcontact angle θ_0 of the drop on the solid surface (Figure 1) through the equation

$$\cos\theta_0 = -b \tag{33}$$

which follows from eq 32 because $x_h|_{h=0} = -\cot\theta_0$. It should be noted that the microcontact angle is obtained from pure microscopic considerations, without involving such thermodynamic quantities as the surface tensions.

The substitution $p = x_h$ transforms eq 26 into the first-order equation

$$\frac{p_h}{(1+p^2)^{3/2}} = \lambda_c + a_1\Phi^l_{LS}(h) \tag{34}$$

which has the solution

$$p = \frac{\Psi(h)}{\sqrt{1-\Psi^2(h)}} \tag{35}$$

where

$$\Psi(h) = \frac{x_h}{\sqrt{1+x_h^2}} = \lambda_c h + D(h) + C \tag{36}$$

$$D(h) = a_1\int\Phi^l_{LS}(h)\,dh \tag{37}$$

and C is a constant of integration. After substitution of x_h instead of p into eq 35, the following general solution for $x(h)$ can be obtained[1]

$$x(h) - x_0 = \int_0^h \frac{\Psi(h)}{\sqrt{1-\Psi^2(h)}}\,dh \tag{38}$$

where $x_0 \equiv x(0)$ (Figure 3) is a second integration constant. It can be determined from the condition for the drop apex to be located on the h-axis [$x(h_m) = 0$], which leads to the expression

$$x_0 = -\int_0^{h_m} \frac{\Psi(h)}{\sqrt{1-\Psi^2(h)}}\,dh \tag{39}$$

The first integration constant, C, can be obtained using the boundary condition eq 32, which is equivalent to the equation $\Psi(0) = b = -\cos\theta_0$. The latter equation provides for C the value $C = b - D(0)$, and the function $\Psi(h)$ becomes

$$\Psi(h) = b + \lambda_c h + D(h) - D(0) \tag{40}$$

After the determination of x_0 and C, the solution, eq 38, still contains two unknown parameters, λ_c and h_m. A connection between them is provided by the boundary condition eq 31, which leads to the equation $\Psi(h_m) = \pm 1$. The sign can be selected by observing that in the absence of liquid−solid interactions a drop must have a spherical shape and contact the solid surface only at $x_0 = 0$. Such a solution can be obtained[1] if $\Psi(h_m) = -1$, which provides the following equation for λ_c:

$$\lambda_c = -\frac{1}{h_m}[1 - \cos\theta_0 + D(h_m) - D(0)] \tag{41}$$

The last necessary condition for the determination of all unknown parameters is provided by the equation for the drop volume, $V = 2\int_0^{h_m} x\,dh$. Integrating by parts and taking into account that $x(h_m) = 0$, one can rewrite the latter equation in the form $V = -2\int_0^{h_m} hx_h\,dh$, which after substitution of expression eq 35 for $x_h = p$ becomes

$$V = -2\int_0^{h_m} \frac{h\Psi(h)}{\sqrt{1-\Psi^2(h)}}\,dh \tag{42}$$

B. Existence of a Cylindrical Drop on a Bare Surface. The first necessary condition for the existence of a drop on a bare surface follows from eq 33 and has the simple form $|b| \le 1$. It establishes [through eq 20] a restriction for the values of the microscopic parameters for which a drop can be formed on a solid surface. If $|b| > 1$, the drop will spread completely over the surface of the solid. It should be noted that this restriction is very different from the traditional one. The latter implies $|\cos\theta_m| > 1$.

Another necessary condition results from the fact that the integral in the right-hand side of eq 38 exists only if the function $\Psi(h)$ satisfies the inequality $|\Psi(h)| < 1$ for $0 < h < h_m$. Because, as shown above, $\Psi(h_m) = -1$, the function $\Psi(h)$ has to be a decreasing one in the vicinity of $h = h_m$, that is, its derivative at that point must be negative

$$\frac{d\Psi(h)}{dh}|_{h=h_m} < 0 \tag{43}$$

This inequality provides a second necessary condition for the existence of a drop on a bare surface.

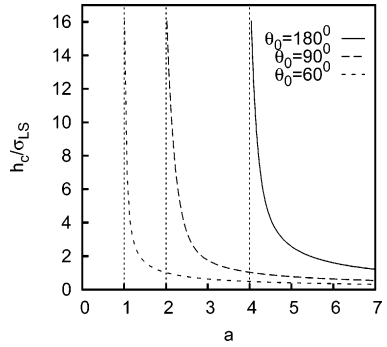

Figure 4. *a*-dependence of the critical height h_c for various values of the microcontact angle from the domain of limited height. The vertical asymptotes for θ_0 equal to 60°, 90°, and 180° are given by equations $a = 1$, $a = 2$, and $a = 4$, respectively.

When expression 40 is used for $\Psi(h)$ and expression 37 is used for $D(h)$, condition 43 becomes

$$\lambda_c + a_1\Phi^l_{LS}(h_m) < 0 \tag{44}$$

which is equivalent to the condition for the drop profile to be convex at the drop apex. Together with eq 41 for λ_c, inequality 44 acquires the form

$$-1 + \cos\theta_0 - D(h_m) + D(0) + a_1\Phi^l_{LS}(h_m) < 0 \tag{45}$$

and provides a restriction for the drop height, h_m, the specific form of which depends on the form of potential $\Phi^l_{LS}(h)$.

B.1. London−van der Waals Potential. In this case, the potential $\Phi^l_{LS}(h)$ is given by eq 7 with $k_\phi = 0$, and inequality 45 can be rewritten as

$$a < A_{LW}(h_m,\theta_0) \tag{46}$$

where

$$a = \frac{4}{3}\frac{\epsilon_{LS}}{\epsilon_{LL}}\frac{\rho_S}{\rho_L}\left(\frac{\sigma_{LS}}{\eta}\right)^4 \tag{47}$$

and

$$A_{LW}(h) = 2(1 - \cos\theta_0)\left(\frac{\sigma_{LS}}{h}\right)^2\frac{(1 + h/\sigma_{LS})^3}{3 + h/\sigma_{LS}} \tag{48}$$

The analysis of inequality 46 shows that it has a solution for any pair (θ_0, a) of values of the parameters θ_0 and a, where $0 < \theta_0 \leq 180°$ and $a > 0$. However, for some pairs the droplet height h_m can have any value, while for other pairs, it is limited by a critical value h_c given by equation

$$A_{LW}(h_c,\theta_0) = a \tag{49}$$

The domain of pairs of the first kind lies in the plane θ_0-a below a critical curve, the equation of which can be obtained from eq 49 in the limit $h_c \to \infty$

$$a = 2(1 - \cos\theta_0) \tag{50}$$

The domain of the pairs of the second kind lies above that curve. In the latter domain

$$a > 2(1 - \cos\theta_0) \tag{51}$$

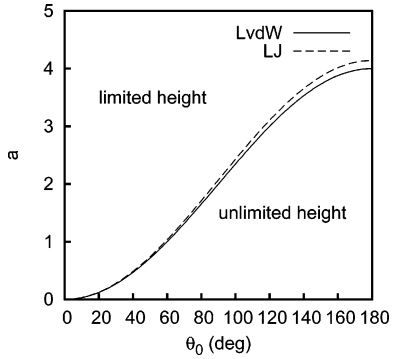

Figure 5. The critical curves in the θ_0-a plane for the LvdW (solid line) and LJ (dashed line) potentials. The domain of limited height for each potential lies above the corresponding critical curve, and the domain of unlimited height lies below it. The points on the critical curves corresponding to $a = 0.8$ have the coordinates θ_0 equal to $\theta_{0,1} = 53.1301°$ and $\theta_{0,2} = 52.1691°$ for the LvdW and LJ potentials, respectively.

The above-mentioned domains and the critical curve (solid line) for the LvdW potential are presented in Figure 5.

The *a*-dependence of h_c provided by eq 49 is presented in Figure 4 for several values of the microcontact angle. For each value of θ_0, there is a critical value a_c of a, near which the height h_c grows rapidly. Obviously, the point (θ_0, a_c) lies on the critical curve [eq 50].

B.2. Lennard-Jones Potential. In this case, inequality 45 acquires the form of inequality 46, where $A_{LW}(h,\theta_0)$ is replaced by

$$A_{LJ}(h,\theta_0) = 60(1 - \cos\theta_0)/[29 - 30(1 + h)^{-2} - 60h(1 + h)^{-3} + (1 + h)^{-8} + 8h(1 + h)^{-9}] \tag{52}$$

The equation for the critical curve, which separates the domains of a and θ_0 in which the height h_m of the drop is limited or unlimited, has the form

$$a = \frac{60}{29}(1 - \cos\theta_0) \simeq 2.07(1 - \cos\theta_0) \tag{53}$$

which is similar to that for the LvdW potential [eq 50]. This curve is presented in Figure 5 by the dashed line. The difference between the critical curves for the LvdW and LJ potentials is small, the value of a for the LJ potential at the same θ_0 being larger than that for the LvdW potential. In the domain in which h_m is limited for both potentials, the value of h_c is larger for the same a and θ_0 for the LJ potential than for the LvdW potential (see Figure 6 plotted for $\theta_0 = 60°$).

C. Shape of the Drop. For the LvdW potential, typical profiles of cylindrical droplets with a constant volume $V/\sigma_{LS}^3 = 4.21 \times 10^4$, but various microcontact angles are presented in Figure 7a for $a = 0.8$ and $x \geq 0$. For this value of a, the drop can have any height for microcontact angles larger that $\theta_{0,1} = 53.1301°$. If $\theta_0 < \theta_{0,1}$, the height is limited. Figure 7a shows that for $\theta_0 > \theta_{0,1}$ the drop height decreases and the half-width x_0 of the contact area of the drop with the solid increases with decreasing microcontact angle. The closer θ_0 is to $\theta_{0,1}$, the larger is x_0, and the drops become almost planar. (This planar drop is not included in Figure 7a because of the very large value of x_0).

As noted earlier in ref 1, the shape of the drop can be often considered circular starting from some distance h_2 from the solid

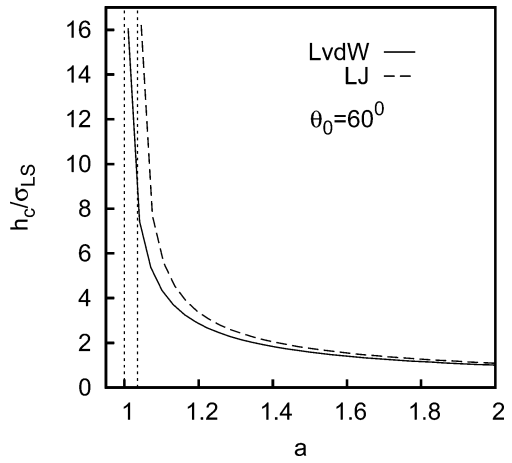

Figure 6. a-dependence of the critical height h_c for the LvdW (solid line) and LJ (dashed line) potentials and for a microcontact angle $\theta_0 = 60°$. The critical values of a are in this case $a_{c,1} = 1$ and $a_{c,2} = 1.035$ for the LvdW and LJ potentials, respectively.

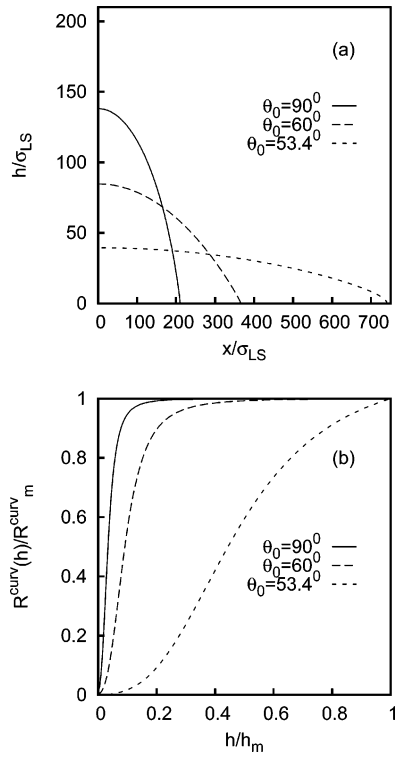

Figure 7. Panel a shows dependence of the drop shape on the microcontact angle for $a = 0.8$. All drops have the same volume $V/\sigma_{LS}^3 \simeq 4.2 \times 10^4$. Panel b shows normalized h-dependence of the curvature radius $R^{curv}(h)$ of the profile for a droplet of volume $V/\sigma_{LS}^3 \simeq 4.2 \times 10^4$ for various microcontact angles. R_m^{curv}/σ_{LS} is equal to 230.3, 845.0, and 8773.0 for θ_0 equal to 90°, 60°, and 53.4°, respectively. R_m^{curv} and h_m are the curvature and height at the apex of the droplet.

surface, that is, for $h_2 < h < h_m$, the curvature radius is almost constant (see Figure 8). In those cases, the circular part of the profile decreases with decreasing microcontact angle. To illustrate this point, which cannot be clearly seen from Figure 7a, the h-dependence of the curvature radius defined by eq 28 is presented in Figure 7b by plotting the normalized values $R^{curv}(h)/R_m^{curv}$ against h/h_m, where $R_m^{curv} \equiv R^{curv}(h_m)$ is the largest value of the curvature radius, which the profile has at the drop apex. One can see that, indeed, the relative range in which $R^{curv}(h)$ can be considered constant is smaller for smaller microcontact angles.

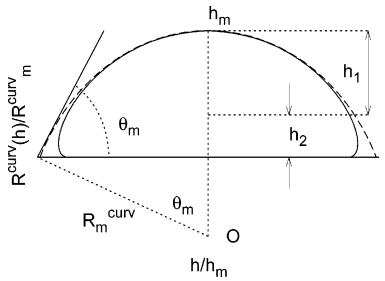

Figure 8. Definition of the macroscopic contact angle θ_m. The dashed line corresponds to the hypothetical circular profile of radius R_m^{curv}, h_1 is the range in which the circular profile almost coincides with the drop profile (solid line), and h_2 is the range of rapid change of the drop profile curvature. The ratio h_2/h_1 has to be small for the macroscopic contact angle to be meaningful.

For large drops, the largest value R_m^{curv} of the curvature radius is a linear function of the drop height

$$R_m^{curv} = h_m(1 - \cos\theta_0 - a/2)^{-1} \tag{54}$$

where $a/2 < 1 - \cos\theta_0$. Equation 54 was obtained by combining eq 28 with eqs 27, 41, and 7 and by considering the limit $h_m/\sigma_{LS} \gg 1$.

Equation 54 can be used to calculate the macroscopic contact angle θ_m, which can be defined (see Figure 8) as the angle between the solid surface and the continuation of the circular part of the profile until its intersection with the surface of the solid. Such a definition is reasonable if the range h_2 of rapid change of the drop curvature is much smaller than the range h_1 where the curvature is almost constant. One can easily see from Figure 8 that θ_m is given by the equation

$$\cos\theta_m = 1 - \frac{h_m}{R_m^{curv}} \tag{55}$$

which, by combination of eqs 54 and 55, becomes

$$\cos\theta_m = \frac{a}{2} + \cos\theta_0 \tag{56}$$

The latter formula provides a connection between the micro- (θ_0) and macrocontact angles (θ_m); it shows that θ_m is always less than θ_0. Indeed, for the profiles presented in Figure 7a, θ_m is equal to 138°, 75.5°, and 41.4° for θ_0 equal to 180°, 90°, and 53.4°, respectively.

If in the above example the microcontact angle θ_0 would acquire values smaller than $\theta_{0,1} = 53.1301°$, then the droplet height would become limited because the pair (θ_0, a) will move into the domain of limited height. The largest possible height h_c depends on θ_0 and decreases rapidly with decreasing θ_0. Indeed, $h_c/\sigma_{LS} = 869.6$ for $\theta_0 = 53.13°$ and $h_c/\sigma_{LS} = 24.4$ for $\theta_0 = 53.0°$. If the drop height at a given θ_0 approaches h_c, the drop becomes planar and its volume grows indefinitely, as in the case $\theta_0 = 180°$ and $a = 4$ considered in ref 1.

For a LJ potential, the shape of the drop has exactly the same peculiarities as for the LvdW potential. However, the corresponding profiles for the same values of a and θ_0 differ in details. Figure 9 presents the profiles of drops of volumes equal to $V/\sigma_{LS}^3 \simeq 2.35 \times 10^5$ for both potentials, $a = 0.8$, and different values of θ_0 in the domain of unlimited height. If the point (a, θ_0) is not close to the critical curves separating the two domains, then the difference between the profiles is not large (the curves of Figure 9 for $\theta_0 = 60°$). However, the difference becomes

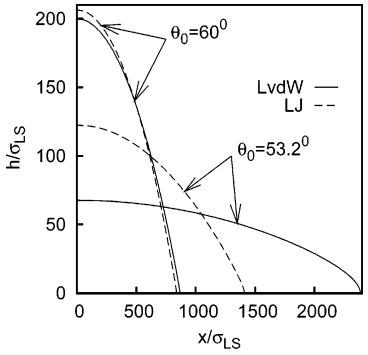

Figure 9. The profiles of a drop of volume $V/\sigma_{LS}^3 \simeq 2.35 \times 10^5$ for the LvdW (solid lines) and LJ (dashed lines) potentials and $a = 0.8$ for two microcontact angles. All the profiles belong to the domain of unlimited height. The values of θ_0 that separate the domains of limited and unlimited heights for $a = 0.8$ are $\theta_{0,1} = 53.1301°$ and $\theta_{0,2} = 52.1691°$ for the LvdW and LJ potentials, respectively.

considerable if that point is in the vicinity of the critical curves (the curves for $\theta_0 = 53.2°$). The reason for such a difference is that, for $a = 0.8$, the smallest possible value of θ_0 from the domain of unlimited droplet height is equal to $\theta_{0,2} = 52.1691°$ for the LJ potential and to $\theta_{0,1} = 53.1301° > \theta_{0,2}$ for the LvdW potential. As already mentioned, the height of the profiles decreases when θ_0 approaches the corresponding smallest value ($\theta_{0,1}$ or $\theta_{0,2}$) at constant a. The closer is θ_0 to $\theta_{0,1}$ ($\theta_{0,2}$), the higher is the rate of decrease. Because $\theta_{0,2} < \theta_{0,1}$, the selected θ_0 is closer to $\theta_{0,1}$ than to $\theta_{0,2}$. Therefore the height of the profile decreases more rapidly for the LvdW potential than for the LJ potential, and as a consequence, the droplet height for the LvdW potential becomes smaller than that for the LJ potential. The physical explanation is that the repulsive part of the LJ potential reduces the effect of the attractive forces between the solid and liquid molecules. This reduction is more effective for small droplet heights (the case of $\theta_0 = 53.2°$) and almost negligible for larger heights ($\theta_0 = 60°$ in our example).

The same features could be observed when the profiles with the same height for LvdW and LJ potentials were compared. Near the critical line, the difference between profiles is very large (Figure 10a), it decreases with increasing θ_0 and becomes almost negligible far from the critical curves (Figure 10b,c).

IV. Axisymmetrical Droplet

If the drop is axisymmetrical with respect to the h-axis, the volume V and the areas of the interfaces are

$$V = \pi\int_0^{h_m} x^2\,\mathrm{d}h, \quad S_{LV} = 2\pi\int_0^{h_m} x\sqrt{1+x_h^2}\,\mathrm{d}h$$

$$S_{LS} = \pi x_0^2 = -2\pi\int_0^{h_m} x x_h\,\mathrm{d}h,$$

$$\int_V \rho_L \Phi_{LS}^l(h)\,\mathrm{d}V = \pi\rho_L\int_0^{h_m} x^2\Phi_{LS}^l(h)\,\mathrm{d}V \quad (57)$$

The total potential energy can be written in the form of eq 18 with

$$f(h,x,x_h) = \frac{\pi^2}{4}\eta^4\rho_L^2\epsilon_{LL}\left[-\frac{a_0}{2}x^2 + x(\sqrt{1+x_h^2} - bx_h) - \frac{a_1}{2}x^2\Phi_{LS}^l(h)\right] \quad (58)$$

where the coefficients a_0, a_1, and b and the function $\Phi_{LS}^l(h)$ are given by expressions 19, 20, and 7, respectively. In this

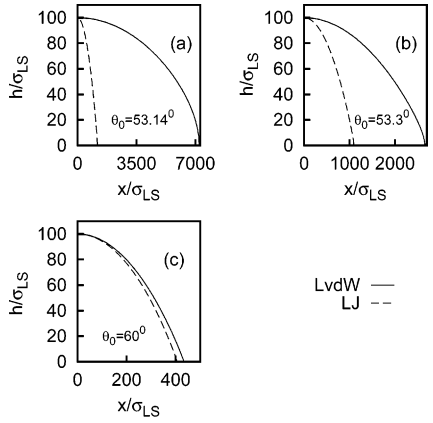

Figure 10. Profiles of cylindrical drops of the same height of the apexes for $a = 0.8$ and various values of the microcontact angle in the domain of unlimited height for the LvdW (solid lines) and LJ (dashed lines) potentials.

case, the Euler equation for the profile has the form

$$\frac{x_{hh}}{(1+x_h^2)^{3/2}} - \frac{1}{x\sqrt{1+x_h^2}} + a_1\Phi_{LS}^l(h) - 2\lambda_a = 0 \quad (59)$$

where λ_a is a Lagrange multiplier. The boundary conditions can be written in the same form as those for cylindrical droplets [eqs 31 and 32] or, equivalently, $x_h|_{h=h_m} = \infty$ ($h_x|_{x=0} = 0$) and $\cos\theta_0 = -b$, where θ_0 is the microcontact angle. Equation 59 cannot be reduced to a first-order differential equation, as for the cylindrical droplets, and therefore all the results presented below have been obtained numerically.

A. Stability of the Axisymmetrical Drop. As for the cylindrical drops (Figure 5), there is a critical curve in the plane θ_0-a that divides the plane into two domains. In one of them (below the critical curve), the height of the drop can have any value, whereas in the other (above the critical curve), the height is limited. Within the precision of the numerical calculations for each potential, LvdW and LJ, the critical curves for axisymmetrical droplets coincide with those for the cylindrical ones. For example, for $a = 0.8$, the critical values of θ_0 for the LvdW potential are equal to $\theta_{c,cyl} = 53.1301°$ and $\theta_{c,a} = 53.1295°$ for the cylindrical and axisymmetrical drops, respectively. For the LJ potential, these values are $\theta_{c,cyl} = 52.1691°$ and $\theta_{c,a} = 52.1690°$, respectively. In the domain of limited heights, the largest possible droplet height h_c for the same a and θ_0 is larger for the axisymmetrical droplet than for the cylindrical one. For example, for $a = 0.8$ and $\theta_0 = 52.1689°$, $h_{c,a} = 1441.9$ and $h_{c,cyl} = 688.1$ for the axisymmetrical and cylindrical droplets, respectively.

B. Shape of the Axisymmetrical Drop. The numerical solution of eq 59 provides the shape of the drop, which is qualitatively similar to that of the cylindrical drop. However, there are quantitative differences, which increase when the pair values (a, θ_0) become closer to the critical curve.

In Figure 11, the profiles of cylindrical and axisymmetrical droplets with the same heights are compared for $a = 0.8$ and various values of θ_0 (the LvdW potential was employed in the calculations) in the domain of unlimited height. Only the profiles for $x \geq 0$ are presented. Far from the critical curve (profiles for $\theta_0 = 60°$), the profiles are almost identical except of a small region near the surface. The macroscopic contact angle for both profiles is equal approximately to 25.9° and remains almost constant when the height of the droplet increases. Therefore, the profile of an axisymmetrical drop far from the critical curve

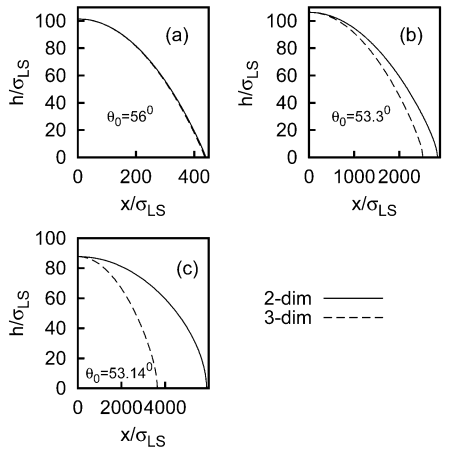

Figure 11. Profiles of the cylindrical (solid lines) and axisymmetrical (dashed lines) droplets of the same height of the apexes for various microcontact angles from the domain of unlimited height for the LvdW potential.

can be represented by the profile of a cylindrical drop, which is much easier to calculate. When θ_0 decreases, the difference between the profiles becomes more pronounced. One can see in the curves for $\theta_0 = 53.3°$ and $\theta_0 = 53.14°$ that the width of the cylindrical drop profile is larger than that of the axisymmetrical one and that both profiles become more planar (the width becoming much larger than the height), when the angle θ_0 decreases. The macroscopic contact angle decreases and becomes very small with decreasing θ_0. For instance, for $\theta_0 = 53.14°$, $\theta_{m,cyl} = 1.37°$ and $\theta_{m,a} = 2.47°$, and for $\theta_0 = 60°$, $\theta_{m,cyl} \simeq \theta_{m,a} \simeq 26.0°$.

For the LJ potential, all the characteristics of the axisymmetrical droplets are qualitatively similar to those for the LvdW potential.

V. Discussion

The analysis of cylindrical and axisymmetrical droplets provided in sections III and IV revealed that their main characteristics are similar. The same similarity was observed with respect to the interaction potential (London−van der Waals or Lennard-Jones potentials). Therefore, the discussion that follows, if not otherwise mentioned, concerns both kinds of drops as well as both kinds of interaction potentials.

The consideration of a monolayer of liquid near a solid surface provided a more realistic description of the characteristics of a drop. The microcontact angle θ_0, which was constant ($\theta_0 = 180°$) in the previous continuum description, ref 1, acquired now a dependence on the microscopic parameters of the model [see eqs 33 and 20], becoming the second parameter that affects the drop features. The first parameter, a, given by eq 47, is also a function of the microscopic parameters of the model (strength of intermolecular interactions, densities of liquid and solid phases, hard core and interaction radius).

Although the microcontact angle is practically undetectable, it influences strongly such drop characteristics as stability, shape, and macroscopic contact angle. One of the consequences of the variability of θ_0 is that instead of a single value a_c of the parameter a, which separates the one-dimensional domain ($a < a_c$) of drops of any height from those ($a > a_c$) in which the height of the drop was limited, there are two two-dimensional domains (Figure 5) in the θ_0-a plane, in which the drops possess those features. Those domains are separated by a critical curve given by eqs 50 and 53. The critical droplet height h_c in the domain of limited height is a function of a and θ_0 and rapidly grows when the point (θ_0, a) approaches the critical curve.

The effect of the microcontact angle θ_0 upon the shape of the drop was illustrated with an example of a drop of a given constant volume. In this case, the relative part of the profile, which can be considered circular, decreases with decreasing θ_0 (Figure 7b). In the domain of limited droplet height, the shape of the drop is planar when its height is close to h_c.

Two stability conditions can be formulated on the basis of the developed theory. The first and strongest condition is that the absolute value of parameter b, eq 20, which is equal to $-\cos \theta_0$, must be not larger than unity. The fulfillment of this condition depends exclusively on the values of the parameters of microscopic liquid−liquid and liquid−solid interactions, which determine the magnitude of b. If $|b| > 1$, no drop can exist on the bare surface, and if created, it has to completely spread on the surface.

The second, weaker stability condition is valid only in the domain of limited droplet height. According to this condition, the droplet height h_m has to be smaller than a critical height h_c, and drops with $h_m > h_c$ cannot exist. If such a drop is created, it has to acquire a shape with a height smaller than h_c.

It seems natural to add to the above two conditions a third one, based on the eq 56 for the macroscopic contact angle θ_m, which also depends on a and θ_0. It follows from that equation that θ_m does not exist if the value $(a/2) + \cos \theta_0$ is larger than unity. This can happen even for small $a > 0$ when the microcontact angle is small and $\cos \theta_0$ is close to unity. However, the nonexistence of the macroscopic contact angle in the considered case does not mean the nonexistence of the drop. Indeed, the inequality $(a/2) + \cos \theta_0 > 1$, which is equivalent to the inequality 51, means only that the pair (θ_0, a) belongs to the domain of limited droplet height in which the large droplets have a planar shape.

The interaction potentials employed provided quantitative differences between the drop profiles, which became more pronounced when the values of the parameters a and θ_0 were near the critical curve. In the latter case, the differences between cylindrical and axisymmetrical droplets were also larger.

Acknowledgment. This work was supported by the National Science Foundation.

References and Notes

(1) Berim, G. O.; Ruckenstein, E. *J. Phys. Chem B*, **2004**, *108*, 19330.
(2) Miller, C. A.; Ruckenstein, E. *J. Colloid Interface Sci.* **1974**, *48*, 368.
(3) Ruckenstein, E.; Lee, P. S. *Surf. Sci.* **1975**, *52*, 298.
(4) Nowakowski, B.; Ruckenstein, E. *J. Phys. Chem.* **1992**, *96*, 2313.
(5) Abraham, F. In *Homogeneous Nucleation Theory*; Academic: New York, 1974.
(6) Lee, S. H.; Rossky, P. J. *J. Phys. Chem.* **1994**, *100*, 3334.
(7) Neimark, A. V. *J. Adhes. Sci. Technol.* **1999**, *13*, 1137.
(8) Sharma, A. *Langmuir* **1993**, *9*, 3580.
(9) Yeh, E. K.; Newman, J.; Radke, C. J. *Colloids Surf.* **1999**, *156*, 137; **1999**, *156*, 525.
(10) Solomentsev, Y.; White, L. R. *J. Colloid Interface Sci.* **1999**, *218*, 122.
(11) McHale, G.; Newton, M. I. *Colloids Surf.* **2002**, *206*, 79.
(12) Elsgolc, L. E. *Calculus of Variations*; Pergamon Press, Addison-Wesley: New York, 1962.